

Thermodynamic Bound on the Asymmetry of Cross-Correlations

Naruo Ohga,^{1,*} Sosuke Ito,^{1,2} and Artemy Kolchinsky²

¹Department of Physics, Graduate School of Science,
The University of Tokyo, 7-3-1 Hongo, Bunkyo-ku, Tokyo 113-0033, Japan

²Universal Biology Institute, Graduate School of Science,
The University of Tokyo, 7-3-1 Hongo, Bunkyo-ku, Tokyo 113-0033, Japan

(Dated: August 24, 2023)

The principle of microscopic reversibility says that, in equilibrium, two-time cross-correlations are symmetric under the exchange of observables. Thus, the asymmetry of cross-correlations is a fundamental, measurable, and often-used statistical signature of deviation from equilibrium. Here we find a simple and universal inequality that bounds the magnitude of asymmetry by the cycle affinity, i.e., the strength of thermodynamic driving. Our result applies to a large class of systems and all state observables, and it suggests a fundamental thermodynamic cost for various nonequilibrium functions quantified by the asymmetry. It also provides a powerful tool to infer affinity from measured cross-correlations, in a different and complementary way to the thermodynamic uncertainty relations. As an application, we prove a thermodynamic bound on the coherence of noisy oscillations, which was previously conjectured by Barato and Seifert [Phys. Rev. E **95**, 062409 (2017)]. We also derive a thermodynamic bound on directed information flow in a biochemical signal transduction model.

One of the most common ways to characterize a physical system is by studying its spatiotemporal correlations. Imagine measuring a pair of observables $a(t)$ and $b(t)$ in a stochastic system in steady state, e.g., 2 degrees of freedom, counts of two chemical species, fluorescence intensity of two colors, voltages of two points, etc. [Fig. 1(a)]. The two-time correlation between a and b at time lag τ is

$$C_{ba}^\tau := \langle b(t + \tau)a(t) \rangle, \quad (1)$$

where $\langle \cdot \rangle$ indicates average across time or trials (it does not depend on t due to the steady-state assumption). When $a = b$, C_{aa}^τ is the autocorrelation function of a . When $a \neq b$, C_{ba}^τ captures the cross-correlation from a to b .

A classic result in statistical physics states that cross-correlations reflect thermodynamic properties of the steady state [1]. In systems without odd degrees of freedom,

cross-correlations in equilibrium obey the symmetry $C_{ba}^\tau = C_{ab}^\tau$ for all a, b , and τ . This is called the principle of microscopic reversibility, and it serves as the basis of the celebrated Onsager reciprocity [1, 2]. Thus, violation of this symmetry is a fundamental and often-used statistical signature of nonequilibrium steady states [3–15].

To maintain a nonequilibrium steady state, a system must be subjected to thermodynamic driving, such as a temperature gradient, a chemical potential gradient, or an external force. In discrete-state stochastic systems as considered here, the strength of different kinds of driving can be quantified in a unified way by the “cycle affinity” [16, 17]. Given a cycle (cyclic sequence of states) c , the cycle affinity \mathcal{F}_c is the sum of the thermodynamic forces acting on the system around the cycle. Equivalently, each time the system completes the cycle, the thermodynamic entropy of the environment increases by \mathcal{F}_c [18]. Cycle affinity vanishes in equilibrium, and it is a fundamental thermodynamic signature of nonequilibrium steady states. Until now, however, these thermodynamic and statistical signatures of deviation from equilibrium have not been universally and quantitatively related.

In this Letter, we prove a universal and simple relationship between asymmetry of cross-correlations and cycle affinity in steady state. To introduce our result, we first define a normalized measure of asymmetry between a and b ,

$$\chi_{ba} := \lim_{\tau \rightarrow 0} \frac{C_{ba}^\tau - C_{ab}^\tau}{2 \sqrt{(\Delta_\tau C_{aa})(\Delta_\tau C_{bb})}}. \quad (2)$$

This measure is dimensionless and invariant under shifting and scaling of observables and time. The normalization terms $\Delta_\tau C_{aa} := C_{aa}^0 - C_{aa}^\tau$ and $\Delta_\tau C_{bb} := C_{bb}^0 - C_{bb}^\tau$ quantify the decay of autocorrelations of a and b [Fig. 1(b)]. They may also be interpreted as measures of diffusion (mean-squared displacements), since $\Delta_\tau C_{aa} = \frac{1}{2} \langle [a(t + \tau) - a(t)]^2 \rangle$.

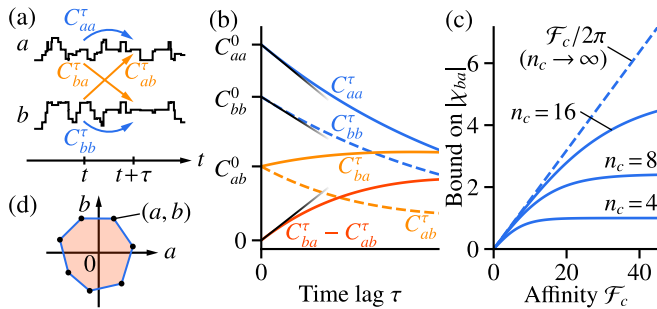


FIG. 1. (a) A pair of observables $a(t)$ and $b(t)$ is measured in a stochastic system in steady state, from which the two-time correlations are calculated. (b) We define a normalized measure of asymmetry of cross-correlation χ_{ba} in Eq. (2) based on the short-time behavior of the correlation functions (black). (c) Our main result is a thermodynamic relation between χ_{ba} and cycle affinity, Eq. (3). (d) The result is derived in part by considering χ_{ba} as the ratio between the area and perimeter of the polygon formed by the values (a, b) over a cycle and then using the isoperimetric inequality.

Our main result is an inequality between cycle affinity and normalized asymmetry between any pair of observables,

$$|\chi_{ba}| \leq \max_c \frac{\tanh(\mathcal{F}_c/2n_c)}{\tan(\pi/n_c)} \leq \max_c \frac{\mathcal{F}_c}{2\pi}, \quad (3)$$

where \max_c is the maximum over all simple cycles and n_c is the number of states in cycle c [see Fig. 1(c)]. The second bound, which refers to cycle affinity per radian, is approached in the limit $n_c \rightarrow \infty$ at a fixed cycle affinity. Some tighter versions of Eq. (3) are provided below.

Our result is physically meaningful and experimentally accessible. It provides a fundamental bound on the asymmetry of cross-correlations achievable at a given level of affinity. This suggests the existence of thermodynamic trade-offs for various physical functions that can be quantified by such asymmetry, including directed interactions and information flow [19–24], nonequilibrium oscillations and circulation [13, 25–30], nonreciprocal motion [31–33], and anomalous response (such as odd viscosity) [34–37].

The normalized asymmetry χ_{ba} is also experimentally accessible, since it depends only on the short-time two-time correlation functions. In fact, χ_{ba} can be expressed in terms of the slopes of auto- and cross-correlation functions, $\chi_{ba} = (\partial_\tau C_{ba}^\tau - \partial_\tau C_{ab}^\tau) / [2\sqrt{(\partial_\tau C_{aa}^\tau)(\partial_\tau C_{bb}^\tau)}]$, where the derivative $\partial_\tau \equiv \partial/\partial\tau$ is evaluated at $\tau = 0$ [Fig. 1(b)]. Such correlations can be measured using, for example, fluorescence cross-correlation spectroscopy [38–40], microscopy [11, 41], and other experimental techniques [42, 43]. In fact, even a single time series can be used if one of the observables is taken to be a nonlinear transformation of the other, such as $b(t) = a(t)^2$. Equation (3) therefore provides a powerful tool for inferring thermodynamic properties from experimental data, in complement to existing techniques like thermodynamic uncertainty relations (TURs) [44–47]. We contrast our bound with TURs below.

The derivation of our result, found at the end of this Letter, combines existing techniques from stochastic thermodynamics with some new ideas. Our most important new idea is to interpret Eq. (2) as the ratio between the area and circumference of the polygon swept out by (appropriately scaled) observables a and b over a cycle [Fig. 1(d)]. We then employ the isoperimetric inequality [48], which says that the area of n -sided polygon with a given circumference is maximized by the regular n -sided polygon [49].

Below, we illustrate our result with a theoretical and a practical application. As a theoretical application, we relate χ_{ba} to the eigenvalues of the rate matrix. This leads to a proof of a thermodynamic bound on the coherence of noisy oscillations, which was previously conjectured by Barato and Seifert [52]. As a practical application, we show that chemical driving force bounds directed information flow in biochemical signal transduction.

System and formulation.—Here we describe our physical setup and define the quantities that appear in our result. We consider a stochastic system modeled as a Markov jump system with a finite number of mesoscopic states $i \in \{1, 2, \dots, n\}$, where the transition rate from state j to i is R_{ij} for $i \neq j$. We define the rate matrix $R \equiv (R_{ij})$ by filling the diagonal elements with $R_{ii} = -\sum_{k:k \neq i} R_{ki}$. The dynamics of the probability distribution $\mathbf{p} = (p_1, \dots, p_n)^T$ obeys $d\mathbf{p}/dt = R\mathbf{p}$. We use \mathbf{q} to indicate a steady-state distribution satisfying $R\mathbf{q} = \mathbf{0}$. For convenience, we use $\mathcal{T}_{ij} = R_{ij}q_j$ to indicate the one-way steady-state flux from j to i (with diagonals $\mathcal{T}_{ii} = R_{ii}q_i \leq 0$).

We define observables a and b to be any functions of the states, denoted by a_i and b_i . In steady state, their cross-correlation at time lag τ can be written as

$$C_{ba}^\tau = \sum_{i,j} (e^{\tau R})_{ij} q_j b_i a_j \approx \sum_i q_i b_i a_i + \tau \sum_{i,j} \mathcal{T}_{ij} b_i a_j, \quad (4)$$

where \approx means equality to first order in τ , which follows by expanding the exponential. The normalization terms in Eq. (2) can be written as

$$\Delta_\tau C_{aa} \approx -\tau \sum_{i,j} \mathcal{T}_{ij} a_i a_j = \frac{\tau}{2} \sum_{i,j} \mathcal{T}_{ij} (a_i - a_j)^2, \quad (5)$$

which follows from $\sum_i \mathcal{T}_{ij} = \sum_j \mathcal{T}_{ij} = 0$. Plugging into (2) gives

$$\chi_{ba} = \frac{\sum_{i,j} \mathcal{T}_{ij} (b_i a_j - b_j a_i)}{2 \sqrt{-\sum_{i,j} \mathcal{T}_{ij} a_i a_j} \sqrt{-\sum_{i,j} \mathcal{T}_{ij} b_i b_j}}. \quad (6)$$

A simple cycle $c = (i_1 \rightarrow i_2 \rightarrow \dots \rightarrow i_{n_c} \rightarrow i_1)$ is a closed path of $n_c \geq 3$ distinct states with $R_{i_{k+1}i_k} > 0$ for $k \in \{1, \dots, n_c\}$ (we use the convention $n_c + 1 \equiv 1$). According to stochastic thermodynamics [16, 17], the cycle affinity \mathcal{F}_c is related to the transition rates by

$$\mathcal{F}_c = \ln \left(\frac{R_{i_2 i_1} R_{i_3 i_2} \dots R_{i_{n_c} i_{n_c-1}}}{R_{i_1 i_2} R_{i_2 i_3} \dots R_{i_{n_c-1} i_{n_c}}} \right). \quad (7)$$

With these definitions, the main result (3) holds. This bound can be saturated, even in systems arbitrarily far from equilibrium. In particular, for a unicyclic system consisting of a single cycle $c = (1 \rightarrow 2 \rightarrow \dots \rightarrow n \rightarrow 1)$, the first (tighter) bound holds with equality if and only if the one-way fluxes are translation invariant, i.e., $\mathcal{T}_{12} = \mathcal{T}_{23} = \dots = \mathcal{T}_{n1}$ and $\mathcal{T}_{21} = \mathcal{T}_{32} = \dots = \mathcal{T}_{1n}$, and there exists a scaling constant γ such that the points $(\gamma a_1, b_1), \dots, (\gamma a_n, b_n)$ form a regular n -sided polygon on the a - b plane in this order.

Tighter bounds.—Under the same setup, we can prove a tighter version of our result,

$$|\chi_{ba}| \leq \max_{c \in C^*} \frac{n_c \tanh(\mathcal{F}_c/2n_c)}{n'_c \tan(\pi/n'_c)} \leq \max_{c \in C^*} \frac{\mathcal{F}_c/2n'_c}{\tan(\pi/n'_c)} \leq \max_{c \in C^*} \frac{\mathcal{F}_c}{2\pi}. \quad (8)$$

Here, n'_c is the number of times the joint value (a, b) changes over course of cycle c , which satisfies $n'_c \leq n_c$. $C^* := C_{\text{asy}} \cap C_{\text{uni}}$ is a restricted set of cycles. C_{asy} is the set of simple cycles $c = (i_1 \rightarrow \dots \rightarrow i_{n_c} \rightarrow i_1)$ that satisfy $\sum_{k=1}^{n_c} (b_{i_{k+1}a_{i_k}} - b_{i_k a_{i_{k+1}}}) \neq 0$, namely, simple cycles with nonzero net asymmetry. This restriction means that cycles with zero net asymmetry cannot contribute to $C_{ba}^\tau - C_{ab}^\tau$, no matter how large \mathcal{F}_c is. C_{uni} is a restricted set of cycles generated by the so-called uniform cycle decomposition [53]. This restriction not only makes the inequality tighter, it also provides a fast algorithm for solving the maximization over cycles. The simpler version (3) is recovered from the first bound in Eq. (8) by using $n'_c \tan(\pi/n'_c) \geq n_c \tan(\pi/n_c)$ and $\max_{c \in C^*}(\cdot) \leq \max_c(\cdot)$. The second bound in (8), which follows from $\tanh(\mathcal{F}_c/2n_c) \leq \mathcal{F}_c/2n_c$, is convenient when n'_c is known but the number of underlying states n_c is unknown.

We can also obtain a tighter result by considering a restricted setup: If the two observables are bipartite, i.e., a and b do not change simultaneously in any transition, then

$$|\chi_{ba}| \leq \max_{c \in C^*} \frac{n_c \tanh(\mathcal{F}_c/2n_c)}{4} \leq \max_{c \in C^*} \frac{\mathcal{F}_c}{8} \leq \max_{c \in C^*} \frac{\mathcal{F}_c}{2\pi}. \quad (9)$$

These bounds may be even tighter than Eq. (8).

Application 1: Coherence of noisy oscillation.—We present a theoretical application of our result by proving a thermodynamic bound on the coherence of noisy oscillation. Noisy oscillations are ubiquitous in biological systems [54, 55], but the oscillation should be coherent in time for reliable biological functionality [56, 57]. Coherence is supported at the cost of dissipation, thus the relation between thermodynamic cost and the coherence of noisy oscillations is actively studied [52, 58–66].

The coherence of oscillation is quantified by the number of oscillations that occur before the steady-state auto-correlations die down. To introduce this, let $\lambda_1, \dots, \lambda_n$ be the eigenvalues of the rate matrix R with real and imaginary parts $\lambda_\alpha = -\lambda_\alpha^R + i\lambda_\alpha^I$. Suppose for simplicity that the rate matrix is diagonalizable, in which case the matrix exponential can be expressed as $e^{\tau R} = \sum_\alpha \exp(-\lambda_\alpha^R \tau) \exp(i\lambda_\alpha^I \tau) \mathbf{u}^{(\alpha)} \mathbf{v}^{(\alpha)\top}$, where $\mathbf{v}^{(\alpha)}$ and $\mathbf{u}^{(\alpha)}$ indicate the left and right eigenvectors of R normalized so that $\mathbf{v}^{(\alpha)\top} \mathbf{u}^{(\alpha)} = 1$. Plugging this expression into Eq. (4) shows that any two-time correlation can be written as a sum over the eigenmodes of R , where the contribution from mode α decays with timescale $(\lambda_\alpha^R)^{-1}$ and oscillates with period $2\pi|\lambda_\alpha^I|^{-1}$. The number of coherent oscillations for mode α is the ratio between the decay time and the period of the oscillations, $(\lambda_\alpha^R)^{-1}/2\pi|\lambda_\alpha^I|^{-1} = |\lambda_\alpha^I|/2\pi\lambda_\alpha^R$ [52, 67].

Barato and Seifert [52] conjectured, based on numerical evidence, that the slowest decay mode (with the smallest nonzero λ_α^R) obeys a thermodynamic bound,

$$\frac{|\lambda_\alpha^I|}{2\pi\lambda_\alpha^R} \leq \max_c \frac{\tanh(\mathcal{F}_c/2n_c)}{2\pi \tan(\pi/n_c)}. \quad (10)$$

This bound implies that coherent oscillations require strong thermodynamic driving. Despite its fundamental and profound nature, this inequality has not been rigorously proven.

Here we use our result (3) to prove that (10) holds for all modes α . We normalize the right eigenvector $\mathbf{u}^{(\alpha)}$ so that $\sum_i |u_i^{(\alpha)}|^2/q_i = 1$ and define two observables $a_i = \text{Im } u_i^{(\alpha)}/q_i$ and $b_i = \text{Re } u_i^{(\alpha)}/q_i$. Using Eqs. (4) and (5), the imaginary and real parts of λ_α can be written as

$$\lambda_\alpha^I = \lim_{\tau \rightarrow 0} \frac{C_{ba}^\tau - C_{ab}^\tau}{\tau}, \quad \lambda_\alpha^R = \lim_{\tau \rightarrow 0} \frac{\Delta_\tau C_{aa} + \Delta_\tau C_{bb}}{\tau}, \quad (11)$$

as derived in the Supplemental Material [68]. Combining Eqs. (11) and (3), together with the inequality $(x+y)/2 \geq \sqrt{xy}$, proves the conjecture (10). The bound (10) is saturated in unicyclic systems with uniform transition rates for the slowest decay mode.

To our knowledge, the expression (11) is new to the literature. More generally, our analytical approach to the eigenvalues of rate matrices complements classical results on this topic [74–79], and it may contribute to ongoing research on the relationship between thermodynamics and complex eigenvalues [60–66]. For instance, Oberreiter *et al.* [65] recently conjectured another thermodynamic bound on $|\lambda_\alpha^I|/2\pi\lambda_\alpha^R$ in terms of entropy production rate. Although our approach alone cannot directly prove this newer conjecture, it may be useful when combined with other ideas.

The result (10) also has practical implications, as it may be used to infer cyclic affinity from empirical observations, assuming some two-time correlation function exhibits a clear damped oscillation corresponding to a particular mode. In this case, one would not directly measure the “observables” a and b , but rather estimate λ_α^I and λ_α^R by fitting the two-time correlation function with a damped oscillation.

Application 2: Signal transduction in a biochemical system.—One of the goals of stochastic thermodynamics is to understand the costs of information processing in biochemical systems [80–90]. To illustrate a practical application of our result, we derive a thermodynamic bound on directed information flow in a standard model of biochemical signal transduction [Fig. 2(a)] [80].

The model consists of an upstream receptor and a downstream protein. The upstream receptor stochastically switches between “OFF” and “ON” states due to ligand binding, corresponding to the observable $a = 0, 1$. The downstream stochastically switches between “0” (inactive) and “1” (active) states, corresponding the observable $b = 0, 1$. When the upstream is ON, the activation of the downstream ($0 \rightarrow 1$) is driven by a chemical force $\Delta\mu > 0$. For example, if the driving is provided by the hydrolysis of a molecule of adenosine triphosphate (ATP), $\Delta\mu = \mu_{\text{ATP}} - \mu_{\text{ADP}} - \mu_{\text{Pi}}$, with μ_X being the environmental chemical potential of X. The bipartite dynamics are

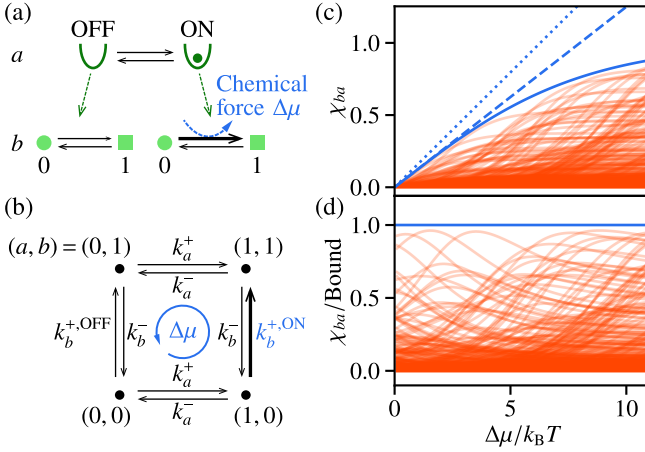


FIG. 2. (a) Simple model of biological signal transduction [80]. (b) Formulation as a Markov jump system with a nonequilibrium cycle. (c) Validation of our bounds. Orange indicates χ_{ba} for varying chemical force $\Delta\mu$, which determines the rate of the transition $k_b^{+,ON}$ (other kinetic rates set to random but fixed values). χ_{ba} is nonnegative for $\Delta\mu \geq 0$ in this model. Blue indicates the three upper bounds from Eq. (12). (d) The ratio between χ_{ba} and the tightest bound $\tanh(\Delta\mu/8k_B T)$ in Eq. (12).

modeled as a four-state Markov jump system depicted in Fig. 2(b). The unique cycle in this system has cycle affinity $\mathcal{F} = \Delta\mu/k_B T$, where k_B is the Boltzmann constant and T is the environmental temperature.

In this model, the cross-correlation C_{ba}^τ is the joint probability of the receptor being ON at time t and the protein being active at time $t + \tau$, and vice versa for C_{ab}^τ . Therefore, the asymmetry $C_{ba}^\tau - C_{ab}^\tau$ provides a simple and natural measure of directed information flow from a to b [19–21]. As for the normalization factor, Eq. (5) implies that $\Delta_\tau C_{aa}$ is one half of the expected number of switching events of a during a short period τ , and similarly for $\Delta_\tau C_{bb}$. Therefore, χ_{ba} is normalized by the frequency of the switches of a and b .

Our general result (8) specializes to

$$|\chi_{ba}| \leq \tanh \frac{\Delta\mu}{8k_B T} \leq \frac{\Delta\mu}{8k_B T} \leq \frac{\Delta\mu}{2\pi k_B T}. \quad (12)$$

See Figs. 2(c) and 2(d). Thus, the chemical force $\Delta\mu$ bounds directed information flow, irrespective of the details of the transition rates. Even if the transition rates are perturbed, the bound is not affected as long as $\Delta\mu$ is unchanged.

Although Eq. (12) was motivated by a specific model of signal transduction [80], the result is much more general. The bound $|\chi_{ba}| \leq \Delta\mu/2\pi k_B T$ applies to any signal transduction system that includes a binary upstream and downstream, including multicyclic systems and systems with nonobserved transition and states, as long as the maximum cycle affinity is $\Delta\mu/k_B T$. The tighter bound $|\chi_{ba}| \leq \Delta\mu/8k_B T$ holds when, in addition, the upstream and

downstream observables are bipartite (do not change at the same time), as follows from Eq. (9).

Derivation.—We sketch the derivation of Eq. (3), restricting our attention to unicyclic systems for simplicity. Further details, including derivation of our tighter bound (8) and consideration of multicyclic systems, are in the Supplemental Material [68].

For each transition $j \rightarrow i$, we define the net probability current $\mathcal{J}_{ij} = \mathcal{T}_{ij} - \mathcal{T}_{ji}$ and the dynamical activity $\mathcal{A}_{ij} = \mathcal{T}_{ij} + \mathcal{T}_{ji}$. We also define $\Omega_{ij} := \frac{1}{2}(b_i a_j - b_j a_i)$ and $L_{ij} := \sqrt{(a_i - a_j)^2 + (b_i - b_j)^2}$.

We recast χ_{ba} in a convenient form. For a unicyclic system with $c = (1 \rightarrow 2 \rightarrow \dots \rightarrow n \rightarrow 1)$, the steady-state currents are uniform, $\mathcal{J}_{21} = \mathcal{J}_{32} = \dots = \mathcal{J}_{1n} =: \mathcal{J}$. We assume without loss of generality that $\mathcal{J} \geq 0$ (otherwise, we may consider the cycle in reverse). Next, since $|\chi_{ba}|$ is invariant under multiplication of a and b by any pair of real numbers, we may assume without loss of generality that a and b are scaled to satisfy $\sum_{i,j} \mathcal{T}_{ij} a_i a_j = \sum_{i,j} \mathcal{T}_{ij} b_i b_j$. Combining this assumption with Eq. (5), we may rewrite the denominator of Eq. (6) as $-\sum_{i,j} \mathcal{T}_{ij} (a_i a_j + b_i b_j) = \frac{1}{2} \sum_{i>j} \mathcal{A}_{ij} L_{ij}^2$. This gives

$$\chi_{ba} = \frac{4\mathcal{J} \sum_i \Omega_{i+1,i}}{\sum_i \mathcal{A}_{i+1,i} L_{i+1,i}^2}. \quad (13)$$

We use two techniques to bound the right side of Eq. (13). First, we generalize the short-time TUR [91] to

$$\frac{(\mathcal{J} \sum_i L_{i+1,i})^2}{\sum_i \mathcal{A}_{i+1,i} L_{i+1,i}^2} \leq \mathcal{J} n \tanh \frac{\mathcal{F}}{2n}, \quad (14)$$

where \mathcal{F} is the cycle affinity of the unique cycle. To prove Eq. (14), we first use the Cauchy–Schwarz inequality to show that the left-hand side is less than $\mathcal{J}^2 \sum_i \mathcal{A}_{i+1,i}^{-1}$. Next, we rewrite the affinity as $\mathcal{F} = 2n \sum_i n^{-1} \text{artanh}(\mathcal{J}/\mathcal{A}_{i+1,i})$ and apply Jensen’s inequality to artanh to show that $\mathcal{J} \sum_i (\mathcal{J}/\mathcal{A}_{i+1,i})$ is less than the right-hand side.

The second technique uses a geometrical interpretation of Ω_{ij} and L_{ij} . $\Omega_{i+1,i}$ is the signed area swept by the observables during the transition $(a_i, b_i) \rightarrow (a_{i+1}, b_{i+1})$, while $L_{i+1,i}$ is the length of this transition [Fig. 1(d)]. Over the course of the cycle, the total signed area is $\sum_i \Omega_{i+1,i}$ and the length of the curve is $\sum_i L_{i+1,i}$. We relate the area and length using the isoperimetric inequality,

$$\left(4n \tan \frac{\pi}{n}\right) \left| \sum_i \Omega_{i+1,i} \right| \leq \left(\sum_i L_{i+1,i} \right)^2. \quad (15)$$

As shown in the Supplemental Material [68], this inequality holds even if the curve has self-intersections. Combining Eqs. (13)–(15) leads to our main result.

Discussion.—In this Letter, we uncovered a universal thermodynamic bound on the asymmetry of cross-correlation between observables. This result holds for any

pair of observables in a finite-state stochastic system in steady state. It is experimentally accessible, relying only on short-time two-point correlation functions.

Our result is similar in spirit to TURs, which also relate the statistical and thermodynamic properties of nonequilibrium steady states [44–47]. However, the two approaches differ both in statistical and thermodynamic aspects. First, our bound is defined using two-time correlations of state observables (e.g., counts of chemical species, voltages, etc.), while TURs are usually defined using the mean and variance of antisymmetric current observables (e.g., chemical reaction fluxes, electric currents, etc.). Although the asymmetry $C_{ba}^r - C_{ab}^r$ can be interpreted as the mean of a specific antisymmetric current observable, the variance of this observable lacks an intuitive physical or statistical interpretation. Second, our bound uses the cycle affinity as the measure of thermodynamic cost, while TURs use the entropy production rate. The affinity is determined by macroscopic parameters (such as environmental chemical potentials) and does not depend on the steady-state distribution. Therefore, it can be interpreted and manipulated at the macroscopic level, and it is robust against microscopic perturbations. In contrast, the entropy production rate captures the resulting dissipation rate and is sensitive to microscopic details. Thus, these two measures provide different and complementary characterizations of the thermodynamic cost. To our knowledge, there is no way to use TURs to bound cycle affinities in general (multicyclic) systems [92].

It is interesting to consider our bound (3) for finite time lags without taking the short-time limit $\lim_{\tau \rightarrow 0}$ in Eq. (2). Given numerical evidence presented in the Supplemental Material [68], we conjecture that our bound holds for all τ . Proving this conjecture is an interesting direction for future work. In addition, future work may generalize our approach to cases when cross-correlations between three or more observables are available at once. Finally, it would be interesting to extend our analysis to continuous-state systems and quantum systems.

We thank Kohei Yoshimura for discussions. N. O. is supported by JSPS KAKENHI Grant No. 23KJ0732. S. I. is supported by JSPS KAKENHI Grants No. 19H05796, No. 21H01560, No. 22H01141, and No. 23H00467, JST ERATO-FS Grant No. JPMJER2204, and UTEC-UTokyo FSI Research Grant Program.

* naruo.ohga@ubi.s.u-tokyo.ac.jp

- [1] H. B. G. Casimir, On Onsager's principle of microscopic reversibility, *Rev. Mod. Phys.* **17**, 343 (1945).
- [2] L. Onsager, Reciprocal relations in irreversible processes. I., *Phys. Rev.* **37**, 405 (1931).
- [3] I. Z. Steinberg, On the time reversal of noise signals, *Biophys.*

- J.* **50**, 171 (1986).
- [4] B. S. Rothberg and K. L. Magleby, Testing for detailed balance (microscopic reversibility) in ion channel gating, *Biophys. J.* **80**, 3025 (2001).
- [5] B. Eckhardt and R. Pandit, Noise correlations in shear flows, *Eur. Phys. J. B* **33**, 373 (2003).
- [6] H. Qian and E. L. Elson, Fluorescence correlation spectroscopy with high-order and dual-color correlation to probe nonequilibrium steady states, *Proc. Natl. Acad. Sci. U.S.A.* **101**, 2828 (2004).
- [7] A. Jachens, J. Schumacher, B. Eckhardt, K. Knobloch, and H. H. Fernholz, Asymmetry of temporal cross-correlations in turbulent shear flows, *J. Fluid Mech.* **547**, 55 (2006).
- [8] C. Paneni, D. J. Searles, and L. Rondoni, Temporal asymmetry of fluctuations in nonequilibrium steady states: Links with correlation functions and nonlinear response, *J. Chem. Phys.* **128**, 164515 (2008).
- [9] K.-H. Choi, M. Tantama, and S. Licht, Testing for violations of microscopic reversibility in ATP-sensitive potassium channel gating, *J. Phys. Chem. B* **112**, 10314 (2008).
- [10] A. Crisanti, A. Puglisi, and D. Villamaina, Nonequilibrium and information: The role of cross correlations, *Phys. Rev. E* **85**, 061127 (2012).
- [11] C. Battle, C. P. Broedersz, N. Fakhri, V. F. Geyer, J. Howard, C. F. Schmidt, and F. C. MacKintosh, Broken detailed balance at mesoscopic scales in active biological systems, *Science* **352**, 604 (2016).
- [12] J. Gladrow, C. P. Broedersz, and C. F. Schmidt, Nonequilibrium dynamics of probe filaments in actin-myosin networks, *Phys. Rev. E* **96**, 022408 (2017).
- [13] A. Ghanta, J. C. Neu, and S. Teitworth, Fluctuation loops in noise-driven linear dynamical systems, *Phys. Rev. E* **95**, 032128 (2017).
- [14] F. Mura, G. Gradziuk, and C. P. Broedersz, Nonequilibrium Scaling Behavior in Driven Soft Biological Assemblies, *Phys. Rev. Lett.* **121**, 038002 (2018).
- [15] D. Brogioli, F. Croccolo, and A. Vailati, Asymmetric time-cross-correlation of nonequilibrium concentration fluctuations in a ternary liquid mixture, *Phys. Rev. E* **99**, 053115 (2019).
- [16] J. Schnakenberg, Network theory of microscopic and macroscopic behavior of master equation systems, *Rev. Mod. Phys.* **48**, 571 (1976).
- [17] U. Seifert, Stochastic thermodynamics, fluctuation theorems and molecular machines, *Rep. Prog. Phys.* **75**, 126001 (2012).
- [18] We treat entropy as dimensionless by dividing it by the Boltzmann constant k_B .
- [19] G. Nolte, F. C. Meinecke, A. Ziehe, and K.-R. Müller, Identifying interactions in mixed and noisy complex systems, *Phys. Rev. E* **73**, 051913 (2006).
- [20] D. Sisan, D. Yarar, C. Waterman, and J. Urbach, Event ordering in live-cell imaging determined from temporal cross-correlation asymmetry, *Biophys. J.* **98**, 2432 (2010).
- [21] S. S. Borysov and A. V. Balatsky, Cross-correlation asymmetries and causal relationships between stock and market risk, *PLoS One* **9**, e105874 (2014).
- [22] L. Kullmann, J. Kertész, and K. Kaski, Time-dependent cross-correlations between different stock returns: A directed network of influence, *Phys. Rev. E* **66**, 026125 (2002).
- [23] S. Haufe, V. V. Nikulin, K.-R. Müller, and G. Nolte, A critical assessment of connectivity measures for EEG data: A simulation study, *NeuroImage* **64**, 120 (2013).
- [24] X. Qin, E. Hannezo, T. Mangeat, C. Liu, P. Majumder, J. Liu, V. Choemmel-Cadamuro, J. A. McDonald, Y. Liu, B. Yi, and X. Wang, A biochemical network controlling basal myosin os-

- cillation, *Nat. Commun.* **9**, 1210 (2018).
- [25] K. Tomita and H. Tomita, Irreversible circulation of fluctuation, *Prog. Theor. Phys.* **51**, 1731 (1974).
- [26] H. Qian, S. Saffarian, and E. L. Elson, Concentration fluctuations in a mesoscopic oscillating chemical reaction system, *Proc. Natl. Acad. Sci.* **99**, 10376 (2002).
- [27] F. S. Gnesotto, F. Mura, J. Gladrow, and C. P. Broedersz, Broken detailed balance and non-equilibrium dynamics in living systems: a review, *Rep. Prog. Phys.* **81**, 066601 (2018).
- [28] J. P. Gonzalez, J. C. Neu, and S. W. Teitsworth, Experimental metrics for detection of detailed balance violation, *Phys. Rev. E* **99**, 022143 (2019).
- [29] K. Yasuda and S. Komura, Nonreciprocity of a micromachine driven by a catalytic chemical reaction, *Phys. Rev. E* **103**, 062113 (2021).
- [30] S. Teitsworth and J. C. Neu, Stochastic line integrals and stream functions as metrics of irreversibility and heat transfer, *Phys. Rev. E* **106**, 024124 (2022).
- [31] R. Golestanian and A. Ajdari, Analytic results for the three-sphere swimmer at low Reynolds number, *Phys. Rev. E* **77**, 036308 (2008).
- [32] R. Golestanian and A. Ajdari, Stochastic low Reynolds number swimmers, *J. Phys. Condens. Matter* **21**, 204104 (2009).
- [33] M. Tarama and R. Yamamoto, Mechanics of cell crawling by means of force-free cyclic motion, *J. Phys. Soc. Jpn.* **87**, 044803 (2018).
- [34] M. Evans, Symmetry analysis of non-equilibrium time correlation functions, *Mol. Phys.* **67**, 1195 (1989).
- [35] J. M. Epstein and K. K. Mandadapu, Time-reversal symmetry breaking in two-dimensional nonequilibrium viscous fluids, *Phys. Rev. E* **101**, 052614 (2020).
- [36] C. Hargus, K. Klymko, J. M. Epstein, and K. K. Mandadapu, Time reversal symmetry breaking and odd viscosity in active fluids: Green-Kubo and NEMD results, *J. Chem. Phys.* **152**, 201102 (2020).
- [37] K. Yasuda, K. Ishimoto, A. Kobayashi, L.-S. Lin, I. Sou, Y. Hosaka, and S. Komura, Time-correlation functions for odd Langevin systems, *J. Chem. Phys.* **157**, 095101 (2022).
- [38] M. Eigen and R. Rigler, Sorting single molecules: Application to diagnostics and evolutionary biotechnology, *Proc. Natl. Acad. Sci. U.S.A.* **91**, 5740 (1994).
- [39] P. Schwille, F. Meyer-Almes, and R. Rigler, Dual-color fluorescence cross-correlation spectroscopy for multicomponent diffusional analysis in solution, *Biophys. J.* **72**, 1878 (1997).
- [40] E. L. Elson, Fluorescence correlation spectroscopy: Past, present, future, *Biophys. J.* **101**, 2855 (2011).
- [41] É. Roldán, J. Barral, P. Martin, J. M. Parrondo, and F. Jülicher, Quantifying entropy production in active fluctuations of the hair-cell bundle from time irreversibility and uncertainty relations, *New J. Phys.* **23**, 083013 (2021).
- [42] K. Ishii and T. Tahara, Two-dimensional fluorescence lifetime correlation spectroscopy. 1. Principle, *J. Phys. Chem. B* **117**, 11414 (2013).
- [43] S. Talele and J. T. King, Reaction cycle of operating pump protein studied with single-molecule spectroscopy, *ChemPhysChem* **23** (2022).
- [44] A. C. Barato and U. Seifert, Thermodynamic Uncertainty Relation for Biomolecular Processes, *Phys. Rev. Lett.* **114**, 158101 (2015).
- [45] T. R. Gingrich, G. M. Rotskoff, and J. M. Horowitz, Inferring dissipation from current fluctuations, *J. Phys. A* **50**, 184004 (2017).
- [46] U. Seifert, From stochastic thermodynamics to thermodynamic inference, *Annu. Rev. Condens. Matter Phys.* **10**, 171 (2019).
- [47] J. M. Horowitz and T. R. Gingrich, Thermodynamic uncertainty relations constrain non-equilibrium fluctuations, *Nat. Phys.* **16**, 15 (2020).
- [48] R. Osserman, The isoperimetric inequality, *Bull. Am. Math. Soc.* **84**, 1182 (1978).
- [49] Other applications of isoperimetric inequality to thermodynamics are found in Refs. [50, 51].
- [50] A. G. Frim and M. R. DeWeese, Geometric Bound on the Efficiency of Irreversible Thermodynamic Cycles, *Phys. Rev. Lett.* **128**, 230601 (2022).
- [51] O. Movilla Miangolarra, A. Taghvaei, Y. Chen, and T. T. Georgiou, Geometry of finite-time thermodynamic cycles with anisotropic thermal fluctuations, *IEEE Control Syst. Lett.* **6**, 3409 (2022).
- [52] A. C. Barato and U. Seifert, Coherence of biochemical oscillations is bounded by driving force and network topology, *Phys. Rev. E* **95**, 062409 (2017).
- [53] P. Pietzonka, A. C. Barato, and U. Seifert, Affinity- and topology-dependent bound on current fluctuations, *J. Phys. A* **49**, 34LT01 (2016).
- [54] J. E. Ferrell, T. Y.-C. Tsai, and Q. Yang, Modeling the cell cycle: Why do certain circuits oscillate?, *Cell* **144**, 874 (2011).
- [55] A. Goldbeter, Biological rhythms: Clocks for all times, *Curr. Biol.* **18**, R751 (2008).
- [56] N. Barkai and S. Leibler, Circadian clocks limited by noise, *Nature* **403**, 267 (2000).
- [57] P. Gaspard, The correlation time of mesoscopic chemical clocks, *J. Chem. Phys.* **117**, 8905 (2002).
- [58] Y. Cao, H. Wang, Q. Ouyang, and Y. Tu, The free-energy cost of accurate biochemical oscillations, *Nat. Phys.* **11**, 772 (2015).
- [59] B. Nguyen, U. Seifert, and A. C. Barato, Phase transition in thermodynamically consistent biochemical oscillators, *J. Chem. Phys.* **149**, 045101 (2018).
- [60] L. Oberreiter, U. Seifert, and A. C. Barato, Subharmonic oscillations in stochastic systems under periodic driving, *Phys. Rev. E* **100**, 012135 (2019).
- [61] C. del Junco and S. Vaikuntanathan, High chemical affinity increases the robustness of biochemical oscillations, *Phys. Rev. E* **101**, 012410 (2020).
- [62] C. del Junco and S. Vaikuntanathan, Robust oscillations in multicyclic Markov state models of biochemical clocks, *J. Chem. Phys.* **152**, 055101 (2020).
- [63] B. Remlein, V. Weissmann, and U. Seifert, Coherence of oscillations in the weak-noise limit, *Phys. Rev. E* **105**, 064101 (2022).
- [64] M. Uhl and U. Seifert, Affinity-dependent bound on the spectrum of stochastic matrices, *J. Phys. A* **52**, 405002 (2019).
- [65] L. Oberreiter, U. Seifert, and A. C. Barato, Universal minimal cost of coherent biochemical oscillations, *Phys. Rev. E* **106**, 014106 (2022).
- [66] A. Kolchinsky, N. Ohga, and S. Ito, Thermodynamic bound on spectral perturbations, *arXiv preprint arXiv:2304.01714* (2023).
- [67] H. Qian and M. Qian, Pumped Biochemical Reactions, Nonequilibrium Circulation, and Stochastic Resonance, *Phys. Rev. Lett.* **84**, 2271 (2000).
- [68] See Supplemental Material at [URL] for the details of the derivation, which includes Refs. [69–73].
- [69] T. Radó, The isoperimetric inequality and the Lebesgue definition of surface area, *Trans. Am. Math. Soc.* **61**, 530 (1947).
- [70] T. Radó, A lemma on the topological index, *Fund. Math.* **1**, 212 (1936).
- [71] P. R. Scott, On a family of polygons, *Math. Mag.* **55**, 104 (1982).
- [72] I. Fáry and E. Makai Jr, Isoperimetry in variable metric, *Stud. Sci. Math. Hung.* **17**, 143 (1982).

- [73] K. Fan, O. Taussky, and J. Todd, An algebraic proof of the isoperimetric inequality for polygons, *J. Wash. Acad. Sci.* **45**, 339 (1955).
- [74] S. Geršgorin, Über die abgrenzung der eigenwerte einer matrix, *Izv. Akad. Nauk. USSR Otd. Fiz.-Mat. Nauk* **6**, 749 (1931).
- [75] N. Dmitriev and E. Dynkin, On the characteristic numbers of a stochastic matrix, *C. R. (Dokl.) Acad. Sci. URSS* **49**, 159 (1945).
- [76] N. Dmitriev and E. Dynkin, On characteristic roots of stochastic matrices, *Izv. Akad. Nauk SSSR Ser. Mat.* **10**, 167 (1946).
- [77] F. I. Karpelevich, On the characteristic roots of matrices with non-negative elements, *Izv. Akad. Nauk SSSR Ser. Mat.* **15**, 361 (1951).
- [78] J. Swift, The location of characteristic roots of stochastic matrices, M.Sc. thesis, *Department of Mathematics and Statistics, McGill University* (1972).
- [79] R. A. Horn and C. R. Johnson, *Matrix Analysis* (Cambridge University Press, Cambridge, 2012).
- [80] P. Mehta and D. J. Schwab, Energetic costs of cellular computation, *Proc. Natl. Acad. Sci. U.S.A.* **109**, 17978 (2012).
- [81] G. Lan, P. Sartori, S. Neumann, V. Sourjik, and Y. Tu, The energy–speed–accuracy trade-off in sensory adaptation, *Nat. Phys.* **8**, 422 (2012).
- [82] A. C. Barato, D. Hartich, and U. Seifert, Information-theoretic versus thermodynamic entropy production in autonomous sensory networks, *Phys. Rev. E* **87**, 042104 (2013).
- [83] S. Ito and T. Sagawa, Information Thermodynamics on Causal Networks, *Phys. Rev. Lett.* **111**, 180603 (2013).
- [84] C. C. Govern and P. R. ten Wolde, Energy Dissipation and Noise Correlations in Biochemical Sensing, *Phys. Rev. Lett.* **113**, 258102 (2014).
- [85] C. C. Govern and P. R. Ten Wolde, Optimal resource allocation in cellular sensing systems, *Proc. Natl. Acad. Sci. U.S.A.* **111**, 17486 (2014).
- [86] A. C. Barato, D. Hartich, and U. Seifert, Efficiency of cellular information processing, *New J. Phys.* **16**, 103024 (2014).
- [87] P. Sartori, L. Granger, C. F. Lee, and J. M. Horowitz, Thermodynamic costs of information processing in sensory adaptation, *PLoS Comput. Biol.* **10**, e1003974 (2014).
- [88] P. R. ten Wolde, N. B. Becker, T. E. Ouldridge, and A. Mugler, Fundamental limits to cellular sensing, *J. Stat. Phys.* **162**, 1395 (2016).
- [89] S. Ito and T. Sagawa, Maxwell’s demon in biochemical signal transduction with feedback loop, *Nat. Commun.* **6**, 7498 (2015).
- [90] P. Mehta, A. H. Lang, and D. J. Schwab, Landauer in the age of synthetic biology: Energy consumption and information processing in biochemical networks, *J. Stat. Phys.* **162**, 1153 (2016).
- [91] S. Otsubo, S. Ito, A. Dechant, and T. Sagawa, Estimating entropy production by machine learning of short-time fluctuating currents, *Phys. Rev. E* **101**, 062106 (2020).
- [92] Inequalities on cycle affinities in terms of cycle-based statistics [93] and waiting-time statistics [94] have recently been proposed. However, these inequalities cannot be used to study the asymmetry of cross-correlations.
- [93] M. Poletini, G. Falasco, and M. Esposito, Tight uncertainty relations for cycle currents, *Phys. Rev. E* **106**, 064121 (2022).
- [94] J. van der Meer, B. Ertel, and U. Seifert, Thermodynamic Inference in Partially Accessible Markov Networks: A Unifying Perspective from Transition-Based Waiting Time Distributions, *Phys. Rev. X* **12**, 031025 (2022).

Supplemental Material for Thermodynamic Bound on the Asymmetry of Cross-Correlations

Naruo Ohga, Sosuke Ito, and Artemy Kolchinsky

In Sec. A, we prove the expression of eigenvalues in Eq. (11). In Sec. B, we provide the full derivation of our main results and the tighter versions, Eqs. (3), (8) and (9), for general multicyclic systems. In Sec. C, we show numerical evidence that supports the finite- τ version of our bound. In Sec. D, we provide supplemental discussions, such as implicit assumptions made in the main text and the equality conditions.

A. Proof of the expressions of eigenvalues in Eq. (11)

We prove the expression of λ_α^R and λ_α^I by two-time correlations in Eq. (11), which applies to any of the eigenvalues. For conciseness, we fix an α and omit the suffix α in λ_α and $u_i^{(\alpha)}$ below.

Proof Eq. (11).—Thanks to the special normalization of the eigenvector, $\sum_i |u_i|^2/q_i = 1$, we can rewrite the eigenvalue λ as

$$\lambda = \sum_i \frac{u_i^*}{q_i} \lambda u_i = \sum_{i,j} \frac{u_i^*}{q_i} R_{ij} u_j = \sum_{i,j} R_{ij} q_j \frac{u_i^*}{q_i} \frac{u_j}{q_j}. \quad (\text{S1})$$

Using the definition $\mathcal{T}_{ij} = R_{ij} q_j$ and the observables $a_i = \text{Im } u_i/q_i$ and $b_i = \text{Re } u_i/q_i$ introduced in the main text, we obtain

$$\begin{aligned} \lambda &= \sum_{i,j} \mathcal{T}_{ij} (b_i - i a_i)(b_j + i a_j), \\ &= \sum_{i,j} \mathcal{T}_{ij} (b_i b_j + a_i a_j + i b_i a_j - i a_i b_j). \end{aligned} \quad (\text{S2})$$

Therefore, the real and imaginary parts, $\lambda = -\lambda^R + i\lambda^I$, are given by

$$\lambda^I = \sum_{i,j} \mathcal{T}_{ij} (b_i a_j - a_i b_j) = \lim_{\tau \rightarrow 0} \frac{C_{ba}^\tau - C_{ab}^\tau}{\tau}, \quad (\text{S3})$$

$$\lambda^R = - \sum_{i,j} \mathcal{T}_{ij} (b_i b_j + a_i a_j) = \lim_{\tau \rightarrow 0} \frac{\Delta_\tau C_{aa} + \Delta_\tau C_{bb}}{\tau}, \quad (\text{S4})$$

where we have used the expressions of the correlations in Eqs. (4) and (5). ■

We remark that we can also recast Eq. (S1) in terms of the currents $\mathcal{J}_{ij} = \mathcal{T}_{ij} - \mathcal{T}_{ji}$ and the dynamical activity $\mathcal{A}_{ij} = \mathcal{T}_{ij} + \mathcal{T}_{ji}$ as

$$\lambda^I = \sum_{i>j} \mathcal{J}_{ij} \text{Im} \left(\frac{u_i^* u_j}{q_i q_j} \right), \quad \lambda^R = \frac{1}{2} \sum_{i>j} \mathcal{A}_{ij} \left| \frac{u_i}{q_i} - \frac{u_j}{q_j} \right|^2, \quad (\text{S5})$$

where we have used $\sum_i \mathcal{T}_{ij} = \sum_j \mathcal{T}_{ij} = 0$ to obtain the expression of λ^R . This expression connects the system's global dynamics characterized by the eigenvalues to the local dynamics characterized by \mathcal{J}_{ij} and \mathcal{A}_{ij} : The global oscillation λ^I due to a current along a cycle is governed by the local current \mathcal{J}_{ij} , and the global relaxation λ^R is governed by the local frequency of transitions \mathcal{A}_{ij} .

B. Derivation of the main results

We show the complete proof of our main result (3) and the tighter versions, Eqs. (8) and (9). We use the symbols \mathcal{J}_{ij} , \mathcal{A}_{ij} , Ω_{ij} , and L_{ij} defined in the *Derivation* section in the main text.

The derivation proceeds in the same way as in the derivation for unicyclic systems. We rewrite the measure of asymmetry χ_{ba} in Secs. B 1–B 3, develop two tools in Secs. B 4 and B 5, and finally prove Eqs. (3), (8), and (9) in Sec. B 6.

B.1 Rewriting the ratio χ_{ba}

The first step of the proof is to rewrite χ_{ba} in a convenient form, as has been done in the main text. Since $|\chi_{ba}|$ is invariant under multiplication of a and b by any pair of real numbers, we may assume without loss of generality that a and b are scaled so that

$$\sum_{i,j} \mathcal{T}_{ij} a_i a_j = \sum_{i,j} \mathcal{T}_{ij} b_i b_j. \quad (\text{S6})$$

Under this assumption, we can rewrite χ_{ba} in Eq. (6) as

$$\begin{aligned} \chi_{ba} &= \frac{\sum_{i,j} \mathcal{T}_{ij} (b_i a_j - b_j a_i)}{-\sum_{i,j} \mathcal{T}_{ij} (a_i a_j + b_i b_j)} \\ &= \frac{\sum_{i,j} \mathcal{T}_{ij} (b_i a_j - b_j a_i)}{\frac{1}{2} \sum_{i,j} \mathcal{T}_{ij} [(a_i - a_j)^2 + (b_i - b_j)^2]} \\ &= \frac{4 \sum_{i,j} \mathcal{T}_{ij} \Omega_{ij}}{\sum_{i,j} \mathcal{T}_{ij} L_{ij}^2} \\ &= \frac{4 \sum_{i>j} \mathcal{J}_{ij} \Omega_{ij}}{\sum_{i>j} \mathcal{A}_{ij} L_{ij}^2}, \end{aligned} \quad (\text{S7})$$

where the second equality is due to the second equality in Eq. (5), and the last equality follows from $\Omega_{ij} = -\Omega_{ji}$ and $L_{ij} = L_{ji}$. The absolute value reads

$$|\chi_{ba}| = \frac{4 |\sum_{i>j} \mathcal{J}_{ij} \Omega_{ij}|}{\sum_{i>j} \mathcal{A}_{ij} L_{ij}^2}, \quad (\text{S8})$$

which follows from $\mathcal{A}_{ij} \geq 0$ and $L_{ij} \geq 0$.

B.2 Notation

We introduce notation suitable for analyzing multicyclic systems. We use the symbol $e = (j \rightarrow i)$ to denote the

transition from j to i , which we call a (directed) edge after the terminology in graph theory. For an edge $e = (j \rightarrow i)$, we use the symbol $-e$ to denote the transition in the opposite direction $-e = (i \rightarrow j)$, and we use $\mathcal{T}_e \equiv \mathcal{T}_{ij}$, $\mathcal{T}_{-e} \equiv \mathcal{T}_{ji}$, $\mathcal{J}_e \equiv \mathcal{J}_{ij}$, $\mathcal{A}_e \equiv \mathcal{A}_{ij}$, $\Omega_e \equiv \Omega_{ij}$, and $L_e \equiv L_{ij}$. We define the set of edges with a positive current, $\mathcal{E}^+ := \{e \mid \mathcal{J}_e > 0\}$.

We regard a cycle $c = (i_1 \rightarrow i_2 \rightarrow \dots \rightarrow i_{n_c} \rightarrow i_1)$ as a sequence of edges $(e_1, e_2, \dots, e_{n_c})$ with $e_k = (i_k \rightarrow i_{k+1})$. The summation over the cycle reads $\sum_{e \in c} X_e := \sum_{k=1}^{n_c} X_{e_k}$ for any quantity X_e associated with the edges. In particular, the cycle affinity \mathcal{F}_c in Eq. (7) is rewritten as

$$\mathcal{F}_c = \sum_{k=1}^{n_c} \ln \frac{\mathcal{T}_{i_{k+1}i_k}}{\mathcal{T}_{i_k i_{k+1}}} = \sum_{e \in c} \ln \frac{\mathcal{T}_e}{\mathcal{T}_{-e}}. \quad (\text{S9})$$

B.3 Uniform cycle decomposition

In the steady state, the currents \mathcal{J}_e should not produce any net change of the probability at each state, and thus the currents are written as a superposition of currents that circulate around the cycles. This idea is called the *cycle decomposition* or *Schnakenberg decomposition* [16].

In particular, Ref. [53] shows that there exists a special decomposition with good properties called a *uniform cycle decomposition*. A uniform cycle decomposition employs a subset of simple cycles C_{uni} whose every cycle is aligned with the edge currents, i.e., any edge $e \in c$ for every cycle $c \in C_{\text{uni}}$ belongs to \mathcal{E}^+ . Then, it decomposes the edge currents $\mathcal{J}_e > 0$ for $e \in \mathcal{E}^+$ into positive cycle currents $\mathcal{J}_c > 0$ for $c \in C_{\text{uni}}$ as

$$\mathcal{J}_e = \sum_{c \in C_{\text{uni}}} S_{ec} \mathcal{J}_c, \quad (\text{S10})$$

where $S_{ec} = 1$ for $e \in c$ and $S_{ec} = 0$ for $e \notin c$. Note that $-e \notin c$ for any $e \in \mathcal{E}^+$ and $c \in C_{\text{uni}}$.

Reference [53] discusses an algorithm to find C_{uni} and \mathcal{J}_c . It assigns the edge currents to cycle currents by iterating the following steps: (1) find an edge e^* with the minimum unassigned edge current; (2) pick a cycle c that passes through the edge e^* and is aligned with the edge currents, whose existence is guaranteed; add c to C_{uni} ; (3) set the cycle current $\mathcal{J}_c = \mathcal{J}_{e^*}$; (4) for all $e \in c$, subtract \mathcal{J}_c from the edge currents \mathcal{J}_e and set $S_{ec} = 1$, while for all other edges $e' \notin c$, set $S_{e'c} = 0$. Steps (1)–(4) are repeated until all edge currents are assigned to cycle currents. Although the construction of C_{uni} and \mathcal{J}_c is not necessarily unique, below we fix one out of them.

For any quantity X_e associated with the edges $e \in \mathcal{E}^+$, we obtain

$$\begin{aligned} \sum_{e \in \mathcal{E}^+} \mathcal{J}_e X_e &= \sum_{c \in C_{\text{uni}}} \mathcal{J}_c \left(\sum_{e \in \mathcal{E}^+} S_{ec} X_e \right) \\ &= \sum_{c \in C_{\text{uni}}} \mathcal{J}_c \left(\sum_{e \in c} X_e \right). \end{aligned} \quad (\text{S11})$$

We also have $\mathcal{F}_c > 0$ for $c \in C_{\text{uni}}$ because, in Eq. (S9), the sign of $\ln(\mathcal{T}_e/\mathcal{T}_{-e})$ is the same as the sign of $\mathcal{T}_e - \mathcal{T}_{-e} = \mathcal{J}_e > 0$.

Using a uniform cycle decomposition and Eq. (S11), we can rewrite the numerator of $|\chi_{ba}|$ from Eq. (S8) as

$$\begin{aligned} \left| \sum_{i>j} \mathcal{J}_{ij} \Omega_{ij} \right| &= \left| \sum_{e \in \mathcal{E}^+} \mathcal{J}_e \Omega_e \right| \\ &= \left| \sum_{c \in C_{\text{uni}}} \mathcal{J}_c \left(\sum_{e \in c} \Omega_e \right) \right| \\ &= \left| \sum_{c \in C^*} \mathcal{J}_c \left(\sum_{e \in c} \Omega_e \right) \right| \\ &\leq \sum_{c \in C^*} \mathcal{J}_c \left| \sum_{e \in c} \Omega_e \right|. \end{aligned} \quad (\text{S12})$$

In the third equality, we narrowed the range of the sum from C_{uni} to $C^* = C_{\text{asy}} \cap C_{\text{uni}} = \{c \in C_{\text{uni}} \mid \sum_{e \in c} \Omega_e \neq 0\}$, which is the subset of C_{uni} with the cycles with nonzero net asymmetry, as introduced in the main text. In the fourth line, we used the triangle inequality and $\mathcal{J}_c > 0$. Similarly, the denominator of $|\chi_{ba}|$ from Eq. (S8) is rewritten as

$$\begin{aligned} \sum_{i>j} \mathcal{A}_{ij} L_{ij}^2 &\geq \sum_{e \in \mathcal{E}^+} \mathcal{A}_e L_e^2 \\ &= \sum_{e \in \mathcal{E}^+} \mathcal{J}_e \frac{\mathcal{A}_e}{\mathcal{J}_e} L_e^2 \\ &= \sum_{c \in C_{\text{uni}}} \mathcal{J}_c \left(\sum_{e \in c} \frac{\mathcal{A}_e}{\mathcal{J}_e} L_e^2 \right) \\ &\geq \sum_{c \in C^*} \mathcal{J}_c \left(\sum_{e \in c} \frac{\mathcal{A}_e}{\mathcal{J}_e} L_e^2 \right). \end{aligned} \quad (\text{S13})$$

We have dropped the edges with $\mathcal{J}_{ij} = \mathcal{J}_{ji} = 0$ in the first inequality and further narrowed the range of the sum in the last inequality using that $\mathcal{J}_e > 0$ and $\mathcal{J}_c > 0$ for $e \in c \in C_{\text{uni}}$. In the following, we develop two tools to evaluate these cycle-wise quantities.

B.4 Generalized TUR

The first tool we will use to derive our result is a generalization of the short-time TUR. Compared to the original short-time TUR [91], our generalization uses affinity rather than the entropy production rate, and it deals with each cycle separately.

Lemma.—For any cycle $c \in C_{\text{uni}}$ from a uniform cycle decomposition, and for any quantity X_e associated with the edges $e \in c$,

$$\frac{(\sum_{e \in c} X_e)^2}{\sum_{e \in c} X_e^2 \mathcal{A}_e / \mathcal{J}_e} \leq n_c \tanh \left(\frac{\mathcal{F}_c}{2n_c} \right). \quad (\text{S14})$$

This inequality is saturated if and only if $\mathcal{J}_e/\mathcal{A}_e$ and X_e are each constant across the cycle.

Proof.—We use the Cauchy–Schwarz inequality between vectors $(X_e \sqrt{\mathcal{A}_e/\mathcal{J}_e})_{e \in c}$ and $(\sqrt{\mathcal{J}_e/\mathcal{A}_e})_{e \in c}$ to obtain

$$\frac{(\sum_{e \in c} X_e)^2}{\sum_{e \in c} X_e^2 \mathcal{A}_e/\mathcal{J}_e} \leq \sum_{e \in c} \frac{\mathcal{J}_e}{\mathcal{A}_e}, \quad (\text{S15})$$

where we have used that $\mathcal{J}_e > 0$ for $e \in c$ due to the definition of uniform cycle decomposition. To relate the right-hand side with the cycle affinity, we rewrite the cycle affinity in Eq. (S9) as

$$\begin{aligned} \mathcal{F}_c &= \sum_{e \in c} \ln \frac{\mathcal{J}_e}{\mathcal{F}_c} \\ &= \sum_{e \in c} \ln \frac{\mathcal{A}_e + \mathcal{J}_e}{\mathcal{A}_e - \mathcal{J}_e} \\ &= 2n_c \sum_{e \in c} \frac{1}{n_c} \operatorname{artanh} \left(\frac{\mathcal{J}_e}{\mathcal{A}_e} \right). \end{aligned} \quad (\text{S16})$$

Since $\mathcal{J}_e/\mathcal{A}_e \geq 0$, we can apply Jensen’s inequality to the artanh function in the last line to give

$$\mathcal{F}_c \geq 2n_c \operatorname{artanh} \left(\sum_{e \in c} \frac{1}{n_c} \frac{\mathcal{J}_e}{\mathcal{A}_e} \right). \quad (\text{S17})$$

Inverting this inequality gives

$$\frac{1}{n_c} \sum_{e \in c} \frac{\mathcal{J}_e}{\mathcal{A}_e} \leq \tanh \left(\frac{\mathcal{F}_c}{2n_c} \right). \quad (\text{S18})$$

Combining with Eq. (S15) gives the desired result.

The equality condition for the Cauchy–Schwarz inequality is that the vector $(X_e \sqrt{\mathcal{A}_e/\mathcal{J}_e})_{e \in c}$ is proportional to $(\sqrt{\mathcal{J}_e/\mathcal{A}_e})_{e \in c}$, or equivalently, $X_e \mathcal{A}_e/\mathcal{J}_e$ is uniform along the cycle. The equality condition for the Jensen’s inequality is that $\mathcal{J}_e/\mathcal{A}_e$ is uniform across the cycle. Rearranging these two conditions gives the equality condition in the statement. ■

Note that, when the cycle contains an edge with absolute irreversibility, i.e., $R_{ij} > 0$ and $R_{ji} = 0$, the affinity is $\mathcal{F}_c = \infty$. Equation (S14) still holds formally for such cases.

B.5 Isoperimetric inequality

Next, we prove the other element of the proof, the isoperimetric inequality for polygons. This is a purely mathematical theorem that does not rely on the context. Although the isoperimetric inequality is a well-known result [48], we need to generalize the inequality for possibly self-intersecting polygons, which has not been explicitly stated in literature.

Theorem.—For any sequence of n points $(a_1, b_1), \dots, (a_n, b_n)$ on \mathbb{R}^2 ,

$$\left(4n \tan \frac{\pi}{n} \right) \left| \sum_{i=1}^n \Omega_{i+1,i} \right| \leq \left(\sum_{i=1}^n L_{i+1,i} \right)^2, \quad (\text{S19})$$

where we use the convention $n+1 \equiv 1$. Equality holds if and only if the points $(a_1, b_1), \dots, (a_n, b_n)$ form a regular n -sided polygon of any size on the a – b plane in this order.

Proof.—Let s_i indicate the line segment connecting (a_i, b_i) and (a_{i+1}, b_{i+1}) in the a – b plane. Consider the polygon P formed by the sequence of edges (s_1, \dots, s_n) , which may be non-simple, i.e., self-intersecting. The length of the perimeter of P is given by $L(P) := \sum_i L_{i+1,i}$, and the signed area of a polygon P is defined as $\Omega(P) := \sum_i \Omega_{i+1,i}$ [69]. The signed area has been shown to be equivalent to [section 6.4, 70]

$$\Omega(P) = \iint_{\mathbb{R}^2} w_P(a, b) da db, \quad (\text{S20})$$

where $w_P(a, b)$ is the winding number of the curve P at (a, b) , i.e., the number of times the curve P circulates around the point (a, b) in the clockwise direction subtracted from that in the counter-clockwise direction.

We now define another polygon Q , which is called the “convexification” of P [71, 72]. Q is constructed from the same set of line segments as edges, (s_1, \dots, s_n) , but the edges are translated and permuted so that their angle monotonically increases in a counter-clockwise fashion. Formally, Q is formed by translating and connecting the sequence of edges $(s_{\sigma(1)}, \dots, s_{\sigma(n)})$, where σ is a permutation that guarantees that the angle of the line segment $(a_{\sigma(i)}, b_{\sigma(i)}) - (a_{\sigma(i+1)}, b_{\sigma(i+1)})$ relative to the a axis is monotonically increasing in i .

Since the edges of Q can only increase in angle, Q is convex and simple. For a simple polygon with its edges arranged in the counter-clockwise direction such as Q , $\Omega(Q)$ is the regular geometric area, which obeys the well-known isoperimetric inequality [73],

$$4n \tan(\pi/n) \Omega(Q) \leq L(Q)^2. \quad (\text{S21})$$

Since Q and P have the same number of edges of the same length, $L(Q) = L(P)$. As for the signed area, it has been proved that $\Omega(P) \leq \Omega(Q)$ for the expression of the signed area in Eq. (S20) [Lemma 1, 72]. Plugging these relations into Eq. (S21) gives

$$4n \tan(\pi/n) \Omega(P) \leq L(P)^2. \quad (\text{S22})$$

Next, let P' be the polygon obtained by interchanging a and b from P , which has the signed area $\Omega(P') = -\Omega(P)$ and the perimeter $L(P') = L(P)$. Therefore, Eq. (S22) applied to P' gives

$$-4n \tan(\pi/n) \Omega(P) \leq L(P)^2. \quad (\text{S23})$$

Combining Eqs. (S22) and (S23) gives the desired result (S19).

The isoperimetric inequality for Q (S21) is saturated if and only if Q is regular [73]. The inequality $\Omega(P) \leq \Omega(Q)$ is saturated if and only if P is convex and the edges are

counter-clockwise oriented, or P is contained in a straight line [72]. Therefore, the equality condition of Eq. (S22) is that P is regular, and its edges are counter-clockwise oriented. Similarly, the equality condition of Eq. (S23) is that P is regular, and its edges are clockwise oriented. The equality in Eq. (S19) holds for both of these cases. ■

We note that the statement is purely algebraic, although the proof relies on geometric concepts. A direct consequence of this theorem is the following corollary, which may give a tighter bound.

Corollary.—For a sequence of n points $(a_1, b_1), \dots, (a_n, b_n)$ on \mathbb{R}^2 , let n' be the number of times the joint value (a, b) changes over the cyclic sequence. Formally, n' is the number of labels $i \in \{1, \dots, n\}$ such that $(a_i, b_i) \neq (a_{i+1}, b_{i+1})$, where we use the convention $n+1 \equiv 1$. Then,

$$\left(4n' \tan \frac{\pi}{n'}\right) \left| \sum_{i=1}^n \Omega_{i+1,i} \right| \leq \left(\sum_{i=1}^n L_{i+1,i} \right)^2. \quad (\text{S24})$$

Proof.—This corollary is essentially because the n points form an n' -sided polygon. To prove it formally, Let $I = \{i \in \{1, \dots, n\} \mid (a_i, b_i) \neq (a_{i+1}, b_{i+1})\}$ be the partial set of labels. The size of this set is $|I| = n'$. The isoperimetric inequality (S19) applied to the sequence of points $\{(a_i, b_i) \mid i \in I\}$ (in the increasing order in i) gives

$$\left(4n' \tan \frac{\pi}{n'}\right) \left| \sum_{i \in I} \Omega_{i+1,i} \right| \leq \left(\sum_{i \in I} L_{i+1,i} \right)^2. \quad (\text{S25})$$

On the other hand, since $\Omega_{i+1,i} = 0$ and $L_{i+1,i} = 0$ for $i \notin I$,

$$\sum_{i=1}^n \Omega_{i+1,i} = \sum_{i \in I} \Omega_{i+1,i}, \quad \sum_{i=1}^n L_{i+1,i} = \sum_{i \in I} L_{i+1,i}. \quad (\text{S26})$$

Combining Eqs. (S25) and (S26) proves the desired result. ■

We introduce another Lemma, which will be used for bipartite cases.

Lemma.—Consider a sequence of n points $(a_1, b_1), \dots, (a_n, b_n)$ on \mathbb{R}^2 that satisfies $(a_i - a_{i+1})(b_i - b_{i+1}) = 0$ for $i = 1, \dots, n$. In other words, the value of a and b does not simultaneously change along the sequence. Then,

$$16 \left| \sum_{i=1}^n \Omega_{i+1,i} \right| \leq \left(\sum_{i=1}^n L_{i+1,i} \right)^2. \quad (\text{S27})$$

Proof.—The proof proceeds similarly to the proof of Eq. (S19). We define the edges s_i and the polygon P as in the previous proof. Due to the assumption, the direction of each edge is either 0, $\pi/2$, π , or $3\pi/2$ relative to the a axis.

Let Q be the convexification of P . Then, Q must be a rectangle, and hence satisfy the inequality (S21) with $n = 4$:

$$16 \Omega(Q) \leq L(Q)^2. \quad (\text{S28})$$

As in the previous proof, we have $L(P) = L(Q)$ and $\Omega(P) \leq \Omega(Q)$, and therefore

$$16 \Omega(P) \leq L(P)^2 \quad (\text{S29})$$

holds for P . The proof for $-\Omega(P)$ proceeds similarly to the previous proof. ■

B.6 Proof of the main results

Finally, we combine these tools to finish the proof of Eqs. (3), (8), and (9). Here we explicitly prove the tighter version Eq. (8), which applies to the general setup, and the bipartite case Eq. (9). The simpler version Eq. (3) follows from Eq. (8) by using $n'_c \tan(\pi/n'_c) \geq n_c \tan(\pi/n_c)$ for $n'_c \leq n_c$ and that maximizing over all simple cycles gives a larger result than maximizing over the restricted set C^* .

Proof of Eq. (8).—First, we apply the corollary (S24) of the isoperimetric inequality to the sequence of points $(a_{i_1}, b_{i_1}), \dots, (a_{i_{n_c}}, b_{i_{n_c}})$ for each cycle $c = (i_1 \rightarrow \dots \rightarrow i_{n_c} \rightarrow i_1)$. This gives

$$\left(4n'_c \tan \frac{\pi}{n'_c}\right) \left| \sum_{e \in c} \Omega_e \right| \leq \left(\sum_{e \in c} L_e \right)^2. \quad (\text{S30})$$

We combine Eq. (S30) with Eq. (S12) to obtain

$$\begin{aligned} \left| \sum_{i>j} \mathcal{J}_{ij} \Omega_{ij} \right| &\leq \sum_{c \in C^*} \mathcal{J}_c \left| \sum_{e \in c} \Omega_e \right| \\ &\leq \sum_{c \in C^*} \mathcal{J}_c \left(\sum_{e \in c} L_e \right)^2 \left(4n'_c \tan \frac{\pi}{n'_c} \right)^{-1}, \end{aligned} \quad (\text{S31})$$

where we used that $\mathcal{J}_c > 0$. Next, we combine Eq. (S13) with the generalized TUR (S14) applied to $X_e = L_e$ to rewrite

$$\begin{aligned} \sum_{i>j} \mathcal{A}_{ij} L_{ij}^2 &\geq \sum_{c \in C^*} \mathcal{J}_c \left(\sum_{e \in c} \frac{\mathcal{A}_e}{\mathcal{F}_e} L_e^2 \right) \\ &\geq \sum_{c \in C^*} \mathcal{J}_c \left(\sum_{e \in c} L_e \right)^2 \left(n_c \tanh \frac{\mathcal{F}_c}{2n_c} \right)^{-1}. \end{aligned} \quad (\text{S32})$$

Plugging Eqs. (S31) and (S32) into the expression of χ_{ba} in Eq. (S8) gives

$$|\chi_{ba}| \leq \frac{4 \sum_{c \in C^*} \mathcal{J}_c (\sum_{e \in c} L_e)^2 [4n'_c \tan(\pi/n'_c)]^{-1}}{\sum_{c \in C^*} \mathcal{J}_c (\sum_{e \in c} L_e)^2 [n_c \tanh(\mathcal{F}_c/2n_c)]^{-1}}. \quad (\text{S33})$$

Finally, we use the inequality

$$\frac{\sum_{c \in C^*} y_c}{\sum_{c \in C^*} x_c} \leq \frac{\sum_{c \in C^*} x_c \max_{c \in C^*} \frac{y_c}{x_c}}{\sum_{c \in C^*} x_c} = \max_{c \in C^*} \frac{y_c}{x_c} \quad (\text{S34})$$

for any $x_c \in \mathbb{R}_{>0}$ and $y_c \in \mathbb{R}$, which is saturated if and only if y_c/x_c are equal across all $c \in C^*$. This leads to

$$|\chi_{ba}| \leq \max_{c \in C^*} \frac{4 \mathcal{J}_c (\sum_{e \in c} L_e)^2 [4n'_c \tan(\pi/n'_c)]^{-1}}{\mathcal{J}_c (\sum_{e \in c} L_e)^2 [n_c \tanh(\mathcal{F}_c/2n_c)]^{-1}}$$

$$= \max_{c \in C^*} \frac{n_c \tanh(\mathcal{F}_c/2n_c)}{n'_c \tan(\pi/n'_c)}, \quad (\text{S35})$$

which proves the desired inequality in Eq. (8). ■

Proof of Eq. (9).—Similarly to the proof of Eq. (8), we apply the isoperimetric inequality for bipartite observables, Eq. (S27), to the sequence of points $(a_{i_1}, b_{i_1}), \dots, (a_{i_{n_c}}, b_{i_{n_c}})$ for each cycle $c = (i_1 \rightarrow \dots \rightarrow i_{n_c} \rightarrow i_1)$. This gives

$$16 \left| \sum_{e \in c} \Omega_e \right| \leq \left(\sum_{e \in c} L_e \right)^2. \quad (\text{S36})$$

This is formally equivalent to Eq. (S30) with the replacement of n'_c with 4. Therefore, with the same lines of reasoning as in the previous proof, we obtain Eq. (S35) with the replacement of n'_c with 4. This is identical to the desired result (9). ■

C. Bound for finite time lag τ

While our main result concerns the correlations in the short- τ region, here we conjecture that a similar result holds for any finite τ based on numerical evidence. More precisely, we introduce a finite- τ version of Eq. (2) as

$$\chi_{ba}^\tau = \frac{C_{ba}^\tau - C_{ab}^\tau}{2 \sqrt{(\Delta_\tau C_{aa})(\Delta_\tau C_{bb})}}. \quad (\text{S37})$$

For this ratio, we conjecture

$$|\chi_{ba}^\tau| \leq \max_c \frac{\tanh(\mathcal{F}_c/2n_c)}{\tan(\pi/n_c)} \leq \max_c \frac{\mathcal{F}_c}{2\pi} \quad (\text{S38})$$

for all $\tau > 0$. This conjecture means that the maximum cycle affinity limits the asymmetry of the cross-correlation $C_{ba}^\tau - C_{ab}^\tau$ for all time lags, not just the short- τ regime. Equation (S38) implies the main result (3) by taking the limit $\lim_{\tau \rightarrow 0} \chi_{ba}^\tau = \chi_{ba}$.

To numerically test Eq. (S38), we note that Eq. (S38) for all $\tau > 0$ is equivalent to

$$\sup_{\tau > 0} |\chi_{ba}^\tau| \leq \max_c \frac{\tanh(\mathcal{F}_c/2n_c)}{\tan(\pi/n_c)}. \quad (\text{S39})$$

We plot both sides of Eq. (S39) for 10^6 randomly generated systems in Fig. S1. All the points obey the bound Eq. (S39) without a single exception, which provides numerical evidence to the bound (S39). We leave analytical investigation of this finite- τ bound to future work.

D. Supplemental discussions

D.1 Implicit assumptions

We clarify two assumptions that are implicitly made so that the main results are well-defined. First, the denominator of χ_{ba} should be nonzero, i.e., $\sum_{i,j} \mathcal{T}_{ij} a_i a_j \neq 0$ and

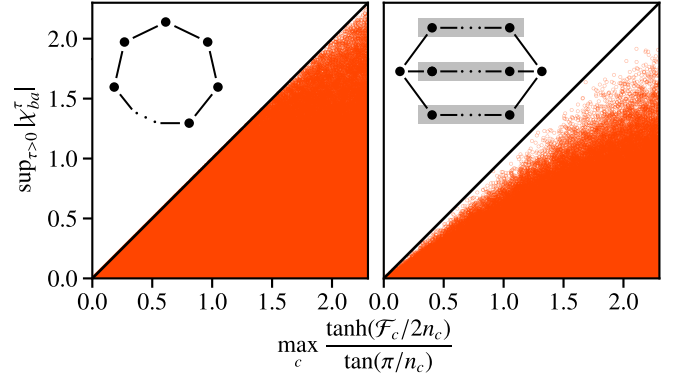


FIG. S1. Numerical evidence for the finite- τ bound (S39) for unicyclic systems (left) and multicyclic systems (right). We generate 10^6 systems with random numbers of states, random transition rates, and random observables a and b , and we plot both sides of Eq. (S39). Insets show the topology of the systems. A circle \bullet denotes a state, and a line $—$ denotes an edge with a nonzero transition rate. The number of states in unicyclic systems (left) are chosen randomly from 3 to 16, and the number of states in each gray-shaded area in multicyclic systems (right) is chosen randomly from 1 to 8.

$\sum_{i,j} \mathcal{T}_{ij} b_i b_j \neq 0$, when we define χ_{ba} . Second, the system should have at least one cycle because otherwise the right-hand side of the result is ill-defined.

These assumptions are not very restrictive because they are automatically satisfied whenever the cross-correlations are asymmetric, $C_{ba}^\tau \neq C_{ab}^\tau$. In other words, if one of these assumptions are violated, it follows that $C_{ba}^\tau = C_{ab}^\tau$. Indeed, if $\sum_{i,j} \mathcal{T}_{ij} a_i a_j = 0$ holds, Eq. (5) shows that $a_i = a_j$ for any pair of i, j with nonzero flux $\mathcal{T}_{ij} \neq 0$. This is equivalent to a being constant along any steady-state trajectory, which leads to $C_{ba}^\tau = C_{ba}^0$. Therefore, the asymmetry is $C_{ba}^\tau - C_{ab}^\tau = C_{ba}^0 - C_{ab}^0 = 0$. Similarly, if $\sum_{i,j} \mathcal{T}_{ij} b_i b_j = 0$ holds, the asymmetry is zero. For a system with no cycles, its steady state is always detailed-balanced, $\mathcal{T}_{ij} = \mathcal{T}_{ji}$ [16]. Therefore, the system has no asymmetry, $C_{ba}^\tau - C_{ab}^\tau = 0$, as confirmed from Eq. (4).

D.2 Rescaling observables

In Sec. B, we have proven our result based on the assumption (S6). Imposing this assumption does not lose generality, as discussed in Sec. B 1, and therefore the proof is already completed. Nevertheless, it will be helpful to give an explicit proof of Eq. (8) for general pair of observables a and b .

Let a and b be any pair of observables that does not necessarily satisfy the assumption (S6). We define a constant

$$\delta = \sqrt{\frac{\sum_{i,j} \mathcal{T}_{ij} b_i b_j}{\sum_{i,j} \mathcal{T}_{ij} a_i a_j}}, \quad (\text{S40})$$

and introduce a new pair of observables $a'_i = \delta a_i$ and $b'_i = b_i$. One can easily confirm the condition $\sum_{i,j} \mathcal{T}_{ij} a'_i a'_j =$

$\sum_{i,j} \mathcal{T}_{ij} b'_i b'_j$, and therefore the above proof applies to the pair a' and b' to deduce

$$|\chi_{b'a'}| \leq \max_{c \in C^*} \frac{n_c \tanh(\mathcal{F}_c/2n_c)}{n'_c \tan(\pi/n'_c)}. \quad (\text{S41})$$

Since $C_{b'a'}^\tau = \delta C_{ba}^\tau$, $C_{a'b'}^\tau = \delta C_{ab}^\tau$, $C_{a'a'}^\tau = \delta^2 C_{aa}^\tau$, and $C_{b'b'}^\tau = C_{bb}^\tau$, it follows that $|\chi_{ba}| = |\chi_{b'a'}|$. Combining this with Eq. (S41) completes the explicit proof of the main result (8).

D.3 Equality conditions

We discuss the equality condition of our main result, Eq. (3), for unicyclic systems.

Proposition.—For unicyclic systems, the first (tighter) inequality in our main result (3) is saturated if and only if (i) \mathcal{A}_e is uniform across the cycle, and (ii) there exist a scaling constant γ such that the points $(\gamma a_1, b_1), \dots, (\gamma a_n, b_n)$ form a regular n -sided polygon in this order.

Proof.—We first find the equality condition under the assumption (S6), and then recast it to the general case.

For a and b obeying the assumption (S6), our main result (3) for unicyclic systems is simply the combination of the generalized TUR and the isoperimetric inequality, as discussed in the main text. By combining their equality conditions, which are stated below Eq. (S14) and Eq. (S19), and noting that the current \mathcal{J}_e is always uniform for unicyclic systems, one can easily find that the equality of Eq. (3) holds if and only if \mathcal{A}_e is uniform across the cycle, and $(a_1, b_1), \dots, (a_n, b_n)$ form a regular n -sided polygon in this order.

For a and b that do not necessarily obey the assumption (S6), the result (3) is obtained by applying the above proof to the rescaled variables $a' = \delta a$ and $b' = b$, as discussed in Sec. D 2. Therefore, the equality condition is that (i) \mathcal{A}_e is uniform along the cycle, and (ii') $(\delta a_1, b_1), \dots, (\delta a_n, b_n)$ form a regular n -sided polygon in this order. It remains to show that the combination of (i) and (ii') is equivalent to the combination of (i) and (ii) in

the statement. We can assume without loss of generality that $\gamma > 0$ because, whenever $(\gamma a_1, b_1), \dots, (\gamma a_n, b_n)$ form a regular n -sided polygon, so do $(-\gamma a_1, b_1), \dots, (-\gamma a_n, b_n)$.

When (i) and (ii') holds, (ii) immediately holds with the choice $\gamma = \delta$. Conversely, suppose that (i) and (ii) are satisfied. Then, the coefficient δ in Eq. (S40) is calculated as

$$\begin{aligned} \delta &= \sqrt{\frac{\sum_i \mathcal{A}_{i+1,i} (b_i - b_{i+1})^2}{\sum_i \mathcal{A}_{i+1,i} (a_i - a_{i+1})^2}} \\ &= \gamma \sqrt{\frac{\sum_i (b_i - b_{i+1})^2}{\sum_i (\gamma a_i - \gamma a_{i+1})^2}} \\ &= \gamma, \end{aligned} \quad (\text{S42})$$

where the first equality is due to Eq. (5), and the second equality is due to the condition (i). The last equality is confirmed by expressing $\gamma a_i = r \cos(i \cdot 2\pi/n + \theta_0)$ and $b_i = r \sin(i \cdot 2\pi/n + \theta_0)$ for any r and θ_0 and calculating

$$\sum_i (b_i - b_{i+1})^2 = \sum_i (\gamma a_i - \gamma a_{i+1})^2 = 2nr^2 \sin^2 \frac{\pi}{n} \quad (\text{S43})$$

using the sum-to-product identities and the power-reduction formulae from trigonometry. Equation (S42) combined with (ii) implies (ii'). ■

Note that the condition (i) is equivalent to the uniformity of the one-way fluxes $\mathcal{T}_{21} = \mathcal{T}_{32} = \dots = \mathcal{T}_{1n}$ and $\mathcal{T}_{12} = \mathcal{T}_{23} = \dots = \mathcal{T}_{n1}$. This is implied by, but not equivalent to, the uniformity of the rates $R_{21} = R_{32} = \dots = R_{1n}$ and $R_{12} = R_{23} = \dots = R_{n1}$.

We can similarly discuss the equality condition for multicyclic systems. For observables that satisfy the assumption (S6), the equality condition is obtained by considering the equality conditions of Eq. (S12), Eq. (S13), the generalized TUR (S14), the isoperimetric inequality (S19), and Eq. (S34). For general observables, we can obtain the equality condition via a rescaling argument as above. We omit further details.